Cellular Oncology (2018) 41:201–212
https://doi.org/10.1007/s13402-017-0366-0

ORIGINAL PAPER

Synergistic anticancer effect of panobinostat and topoisomerase inhibitors through ROS generation and intrinsic apoptotic pathway induction in cervical cancer cells

Lubna Wasim[1] · Madhu Chopra[1]

Accepted: 30 November 2017 / Published online: 19 December 2017

Abstract

Purpose Various combinations of drugs may be effective in the treatment of different types of cancer. Previously, we have shown that combinations of the histone deacetylase inhibitor panobinostat and the topoisomerase inhibitors topotecan or etoposide act synergistically, but the underlying mode of action has remained unknown. Here, we aimed at uncovering the mechanisms underlying this synergism.

Methods The effects of (combinations of) panobinostat and topotecan or etoposide on cervical cancer-derived HeLa and SiHa cells were assessed using morphological evaluations, scratch wound healing assays, cell cycle analyses, AO/EB staining assays, Annexin V/PI staining assays, reactive oxygen species (ROS) and mitochondrial membrane potential measurements and Western blotting.

Results We found that combinations of panobinostat and the topoisomerase inhibitors topotecan or etoposide synergistically enhanced the induction of apoptosis in both HeLa and SiHa cells. This enhanced apoptosis induction was found to be mediated through increased ROS production and induction of the mitochondrial apoptotic pathway. We also found that the combination treatment resulted in inhibition of the PI3K/AKT and NF-κB pro-survival pathways and in activation of the ERK pathway, which is associated with intrinsic apoptosis.

Conclusions From our data we conclude that combinations of panobinostat and the topoisomerase inhibitors topotecan or etoposide provoke strong cell death responses in cervical cancer-derived cells via induction of the intrinsic apoptotic pathway. Since this drug combination may potentially be effective in the treatment of cervical cancer, further preclinical investigations are warranted.

Keywords Combination therapy · Panobinostat · Topoisomerase inhibitors · ROS · Apoptosis · AKT/NF-κB · ERK

1 Introduction

Since the treatment of cancer with conventional chemotherapeutic drugs as monotherapy is associated with side-effects and resistance, combination therapy has recently been explored as a better treatment option [1]. Previous studies have revealed the potential of epigenetic drugs, such as histone deacetylase inhibitors (HDACi), as therapeutic agents for the treatment of both hematological and solid tumors. However, given the pleiotropic effects of HDACi, equivalent responses are not always observed. This notion has encouraged the investigation of treatment combinations, directed against two or more tumor-related mechanisms [2]. As such, HDACi have been shown to be effective in combination with radiation therapy, DNA methylation inhibitors (decitabine, azacitidine), topoisomerase I and II inhibitors (topotecan, doxorubicin, etoposide), cisplatin, anti-tubulin agents (docetaxel, paclitaxel), imanitib (tyrosine kinase inhibitor), bortezomib and carfilzomib (proteasome inhibitors), geldanomycin (heat shock protein-90 inhibitor) and trastuzumab (Her2 receptor inhibitor). Currently, several preclinical and clinical studies on HDACi combination therapies

Electronic supplementary material The online version of this article (https://doi.org/10.1007/s13402-017-0366-0) contains supplementary material, which is available to authorized users.

✉ Madhu Chopra
mchopradu@gmail.com; mchopradu16@gmail.com

Lubna Wasim
lwasim15@gmail.com

[1] Laboratory of Molecular Modeling and Anticancer Drug Development, Dr. B. R. Ambedkar Center for Biomedical Research, University of Delhi, Delhi 110007, India

are ongoing for leukemia, lymphoma, multiple myeloma, lung, breast, ovarian, pancreatic, renal and bladder cancer, neuroblastoma and glioblastoma. HDACi have been shown to induce cell cycle arrest, differentiation and apoptosis in cancer cells [3, 4]. It has been suggested that synergistic interactions between HDACi and DNA damaging agents, such as topoisomerase inhibitors, may be based on close functional interconnections between DNA and chromatin structures during cancer development [5]. The open chromatin structure induced by histone hyperacetylation renders the DNA more accessible to DNA damaging agents, resulting in an increased therapeutic efficacy of the combination [6–8]. Recently, we found via protein-protein interaction analyses that DNA topoisomerase 2-alpha (DNA topo IIα) acts as one of the direct interaction partners of HDAC1 (unpublished data). In addition, we previously reported that the HDACi panobinostat shows anticancer effects on cervical cancer cells and interacts synergistically with the DNA topoisomerase I (topotecan) and II (etoposide) inhibitors in a schedule-dependent manner [9]. Based on these observations, we sought to elucidate the molecular mechanisms underpinning the synergistic anticancer activities of the drug combinations.

Our results show that combinations of panobinostat and the topoisomerase inhibitors topotecan or etoposide synergistically enhance the induction of apoptosis in cervical cancer-derived cells through activation of the intrinsic apoptotic pathway.

2 Materials and methods

2.1 Reagents and antibodies

Panobinostat, topotecan and etoposide were purchased from Selleck Chemicals (Selleck Chemicals, TX, USA). The stock solutions were prepared either in DMSO or in sterile water and kept at −80°C until use. Propidium iodide (PI), 2′, 7′-dichlorodihydrofluorescein diacetate (DCFH-DA), rhodamine 123 (Rh 123), acridine orange (AO), ethidium bromide (EB) and agarose were purchased from Sigma-Aldrich. Antibodies directed against p21, Bax, Bcl-2, Bcl-xL, caspase-9, cleaved PARP, NF-κB, AKT, p-ERK and β-actin were purchased from Santa Cruz Biotechnology (Santa Cruz, CA, USA). Secondary goat anti-rabbit or goat anti-mouse antibodies conjugated to horseradish peroxidase (HRP) were also purchased from Santa Cruz Biotechnology.

2.2 Cell culture and treatment

Human cervical cancer-derived cell lines HeLa and SiHa were purchased from the National Centre for Cell Science (NCCS, Pune, India). These cell lines represent distinct pathological subtypes, i.e., adenocarcinoma, HPV18+ (HeLa) and squamous carcinoma, HPV16+ (SiHa), respectively. Both cell lines were cultured in DMEM (Himedia) supplemented with 10% fetal bovine serum (FBS) and 1% antibiotic-antimycotic solution. The cells were grown in 5% CO_2 at 37°C in a humidified tissue culture incubator and treated with the previously determined [9] $IC_{50}{}^{72h}$ concentrations of panobinostat, topotecan or etoposide, either alone or in combination. HeLa cells were treated with panobinostat (148.4 nM), topotecan (0.75 μM) or etoposide (3.8 μM). Similarly, SiHa cells were treated with panobinostat (52 nM), topotecan (0.11 μM) or etoposide (9 μM). The drugs were applied concurrently in the combination treatment. The cells were harvested after either 24 or 48 h for further analyses.

2.3 Cell morphology analysis

Cells were seeded at a density of 0.3×10^6 in 30 mm culture dishes and treated with $IC_{50}{}^{72h}$ concentrations of panobinostat, topotecan or etoposide, either alone or in combination. Morphological changes were evaluated using an inverted phase-contrast microscope (Nikon Eclipse, Inc., Japan) after 24 h.

2.4 Scratch wound healing assay

To assess cell migration, cells were seeded in 60 mm culture dishes and allowed to attach to the surface under standard incubation conditions. When the cells reached 60–70% confluency, cell monolayers were scratched using a 200 μl sterile pipette tip. Next, the monolayers were carefully rinsed with PBS to remove free-floating cells and cellular debris and incubated in medium with or without drugs after which wound healing was monitored. To this end, the cultures were photographed at 0 and 24 h and marker lines were drawn on the images to analyze the closure of the wound area.

2.5 Cell cycle analysis

HeLa and SiHa cells were treated with $IC_{50}{}^{72h}$ concentrations of panobinostat, topotecan or etoposide, individually or in combination for 24 h. Next, the cells were harvested, washed and fixed with ice-cold 70% (*v*/v) ethanol and stored at −20°C until analysis. For this analysis, cells were centrifuged at 400 g for 5 min, washed and incubated with a DNA staining solution containing PI (20 μg/ml) and DNase-free RNase A (200 μg/ml) at room temperature for 30 min. Next, the DNA content was determined by flow cytometry (FCM) using a FL-2 filter for PI fluorescence (FACS Calibur, BD). Cell cycle analyses were performed using the CellQuest Pro software tool (BD Biosciences, Franklin Lakes, NJ, USA).

2.6 Cell death assays

Acridine orange (AO) and ethidium bromide (EB) double staining assays were performed to visualize cellular changes in response to anti-cancer drugs, such as chromatin condensation and apoptotic body formation, characteristic of apoptosis. Cells were treated with the various drugs (see above), either alone or in combination. After 48 h the cells were washed, pelleted and resuspended, after which a 20 μl aliquot was incubated with 10 μl AO/EB solution. Next, the cells were evaluated under a fluorescence microscope (Nikon Eclipse, Inc., Japan). The samples were processed immediately and all images were captured using the same parameters.

2.7 Apoptosis assays

HeLa and SiHa cells were seeded in 60 mm dishes and incubated overnight. Next, treatment media were added and the cells were incubated for an additional 48 h. Subsequently, both floating and adherent cells were collected and washed in PBS, after which samples were taken to determine drug-induced apoptosis by PI staining or Annexin V/PI double staining using flow cytometry (FACS Calibur; BD Biosciences, Franklin Lakes, NJ, USA). Double staining was performed using an Annexin V Apoptosis Detection Kit APC (eBioscience Inc., CA, USA) according to the manufacturer's protocol. Apoptotic events were expressed as the percent of sub-G1 cells or the percent of apoptotic cells (combining early apoptotic Annexin V^+/PI^- and late apoptotic Annexin V^+/PI^+ cells).

2.8 DNA fragmentation measurement

The extent of nuclear DNA damage by apoptosis was evaluated by measuring the extent of genomic DNA fragmentation. Briefly, treated or untreated cells were harvested after 48 h, after which DNA was extracted and purified using a DNA extraction kit (Qiagen, Chatsworth, CA, USA) according to the manufacturer's protocol. Next, 5–10 μg DNA samples were subjected to electrophoresis in 1% agarose gels containing ethidium bromide and visualized using a GelDoc System.

2.9 Reactive oxygen species measurement

The measurement of reactive oxygen species (ROS) was performed using the cell-permeable probe DCFH-DA. Cells were cultured with media containing $IC_{50}{}^{72h}$ concentrations of panobinostat, topotecan or etoposide, individually or in combination with or without 20 mM NAC (N-acetyl-L-cysteine) for 24 h. Next, the cells were harvested and incubated with 10 μM DCFH-DA for 30 min in the dark after which the fluorescence intensity of the dye was detected in the FL-1 channel of the FACS Calibur. Twenty thousand events were acquired and data were analyzed using the CellQuest Pro software tool.

2.10 Mitochondrial membrane potential analysis

Rhodamine 123 (Rh 123) staining was used to assess (changes in) mitochondrial membrane potential. The transition of mitochondria from a polarized to a depolarized state during the induction of apoptosis results in leakage of the dye which, consequently, results in a decrease in Rh 123 fluorescence intensity. After various drug treatments for 24 h, cells were harvested and incubated with 10 μM Rh 123 for 15 min at 37°C in the dark. Next, the cells were resuspended in PBS and analyzed immediately by flow cytometry (FACS Calibur).

2.11 Western blotting

After drug treatment, the cells were rinsed with ice-cold PBS and lysed in RIPA buffer supplemented with a protease inhibitor cocktail (Sigma-Aldrich). The cell lysates were centrifuged at 14,000 rpm for 10 min at 4°C after which protein concentrations were assayed using a Pierce™ BCA Protein Assay Kit (ThermoFisher Scientific). Next, 20–30 μg of total cell lysate was boiled for 5 min and resolved in 8–12% SDS-polyacrylamide gels by electrophoresis after which the proteins were transferred to polyvinylidene fluoride (PVDF) membranes. The membranes were subsequently blocked with 5% BSA in PBS for 1 h and incubated overnight with the various primary antibodies, typically at a 1:1000 dilution in PBST buffer (0.1% Tween-20) at 4°C. The resulting blots were rinsed with PBST and incubated for 1 h at room temperature with HRP-conjugated secondary antibody at a 1:5000 dilution. Finally, the immune-reactive bands were visualized using an Enhanced Chemiluminescence Kit (Millipore, Germany) in conjunction with an ImageQuant LAS 4000 imaging system (GE Healthcare, Chicago, IL, USA). Band densities were measured and quantified using ImageJ software (NIH, Bethesda, MD, USA).

2.12 Statistical analyses

Statistical analyses were performed using GraphPad Prism 5.0. All measurements were performed in triplicate and each experiment was repeated thrice. The error bars for all data depict the standard deviation (SD) from the mean. Statistical significances between panobinostat, topotecan or etoposide treated (individually or combined) and untreated cells were assessed using Student's t test. A p-value < 0.05 was considered significant.

3 Results

3.1 Induction of morphological changes by combinations of panobinostat and topotecan or etoposide

Previously, we have shown that combinations of panobinostat and the topoisomerase inhibitors topotecan or etoposide have synergistic effects on cervical cancer cells [9]. Here, we investigated the cellular and molecular effects of the combination treatment. Phase-contrast microscopy was performed to study morphological changes induced by combined treatments of panobinostat and the topoisomerase inhibitors in cervical cancer-derived HeLa and SiHa cells. We found that the untreated cells spread regularly in culture and grew to near confluency (Fig. S1, Supplementary file). The cells showed regular oval or polygonal shapes, with few cells showing elongated and almost none showing round shapes. The color was even and the chromatin was loose. Subsequent treatment with IC_{50}^{72h} doses of panobinostat, topotecan or etoposide, alone or in combination for 24 h resulted not only in lower cell densities due to reduced mitotic indices, but also in distinct changes in cellular shape. Single treatment with panobinostat resulted in some floating cells, while the majority of the attached cells exhibited a shrunken shape. Cells incubated with either one of the topoisomerase inhibitors developed an enlarged, flattened-like morphology with long spindle connections between adjacent cells. However, after panobinostat-topoisomerase inhibitor combination treatment a significant proportion of the cells dislodged from the dishes whereas the remaining adherent cells showed shrinkage, loss of adhesion, rounding and an increase in intercellular space, morphological changes that are typical of apoptosis. These results indicate that the concurrent combined drug treatment regimens tested enhance cervical cancer cell killing efficiencies.

3.2 Combinations of panobinostat and topotecan or etoposide inhibit the migration of cervical cancer cells

Next, we investigated the effects of the combined treatment on the migratory capabilities of cervical cancer cells. Using a scratch wound healing assay, we found that the untreated control cells readily migrated and closed the wound gap after 24 h (Fig. 1), whereas the capabilities of the panobinostat or the topoisomerase inhibitors alone and the panobinostat-topoisomerase inhibitor combination treated cells to migrate were significantly reduced. The panobinostat, topotecan or etoposide alone treated cells still showed a tendency to migrate into the scratched wound area, whereas the simultaneous administration of the drugs resulted in a total inhibition of wound healing compared to the control or single drug treated cells. In addition, we noted apoptotic morphological changes such as rounding and membrane blebbing in both cells lines. We conclude that the combined treatment of panobinostat and topotecan or etoposide effectively inhibits the migratory capabilities of the cervical cancer-derived HeLa and SiHa cells.

3.3 Combinations of panobinostat and topotecan or etoposide affect the cell cycle distribution of cervical cancer cells

To determine whether cell cycle arrest represents an additional mechanism driving the synergistic effects observed after combination treatment, cell cycle profiles were assessed in both cell lines treated for 24 h with panobinostat, topotecan or etoposide, alone or in combination. We found that the various tested drugs and their combinations elicited different effects on the cell cycle profiles of both cell lines (Fig. 2). In HeLa cells, panobinostat alone resulted in an arrest at the G0-G1 phase compared to untreated control cells (39.01 to 53.6%). Treatment with either of the two topoisomerase inhibitors resulted in a significant accumulation of the cells in the G2/M phase compared to control cells (topotecan: 21.1 to 85.4%; etoposide: 21.1 to 83.2%) (Fig. 2b). Concomitantly, we found significant decreases in the number of S phase cells in the topotecan (38.3 to 4.6%) and etoposide (38.3 to 6.3%) treated HeLa cells. In contrast, we found that in SiHa cells treatment with panobinostat alone had no effect on G0-G1 phase accumulation compared to untreated control cells (70.51 to 73.2%). Instead, we found that both topoisomerase inhibitors induced prominent S phase arrests in these cells compared to untreated control cells (topotecan: 16.7 to 74.6%; etoposide: 16.7 to 64.7%) (Fig. 2d). Of note, we found that the combined treatment with panobinostat did not alter the cell cycle perturbations induced by topotecan or etoposide in both the HeLa and SiHa cells, but clear increases were noted in the sub-G1 phase populations, indicative of apoptotic effects (Fig. 2a, c). These results indicate that combined panobinostat and topoisomerase inhibitor treatment regimens induce cell cycle perturbations in cervical cancer cells.

3.4 Apoptosis is induced by combined panobinostat and topoisomerase inhibitor treatment

In order to substantiate the above observations on apoptosis induction, the occurrence of putative apoptotic changes was first assessed by AO/EB fluorescence staining of the cells after treatment with panobinostat and the topoisomerase inhibitors, alone or in combination, (Fig. S2). The control cells appeared to have an intact oval shape and were uniformly stained pale-green by AO, indicative

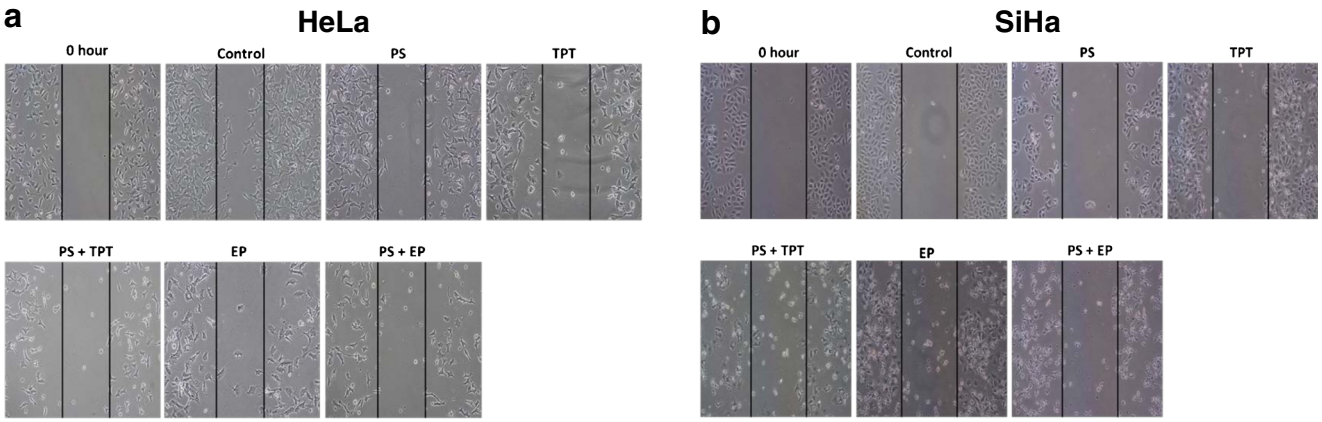

Fig. 1 Wound healing responses of cervical cancer cell lines after exposure to combination treatment of panobinostat and topoisomerase inhibitors. Scratch wounded HeLa (**a**) and SiHa (**b**) cells were incubated with IC_{50}^{72h} doses of various drugs alone or in combination for 24 h. Migrating cells were photographed using a phase-contrast microscope. Images were analyzed by digitally drawing lines (Adobe Photoshop) highlighting the positions of the migrating cells at the wound edges. *PS*, panobinostat; *TPT*, topotecan; *EP*, etoposide

of viability (Fig. S2a, b). Treatment with panobinostat, topotecan or etoposide alone revealed, in addition to viable cells, also bright green cells with intense green dots at the center indicative of chromatin condensation and nuclear fragmentation, which is a typical sign of early apoptosis. In addition, we found that combined treatment of the cells with panobinostat and topotecan or etoposide resulted in mixed populations of both early and late apoptotic cells. The numbers of late apoptotic cells, showing intense yellow-orange or orange-red staining, were higher

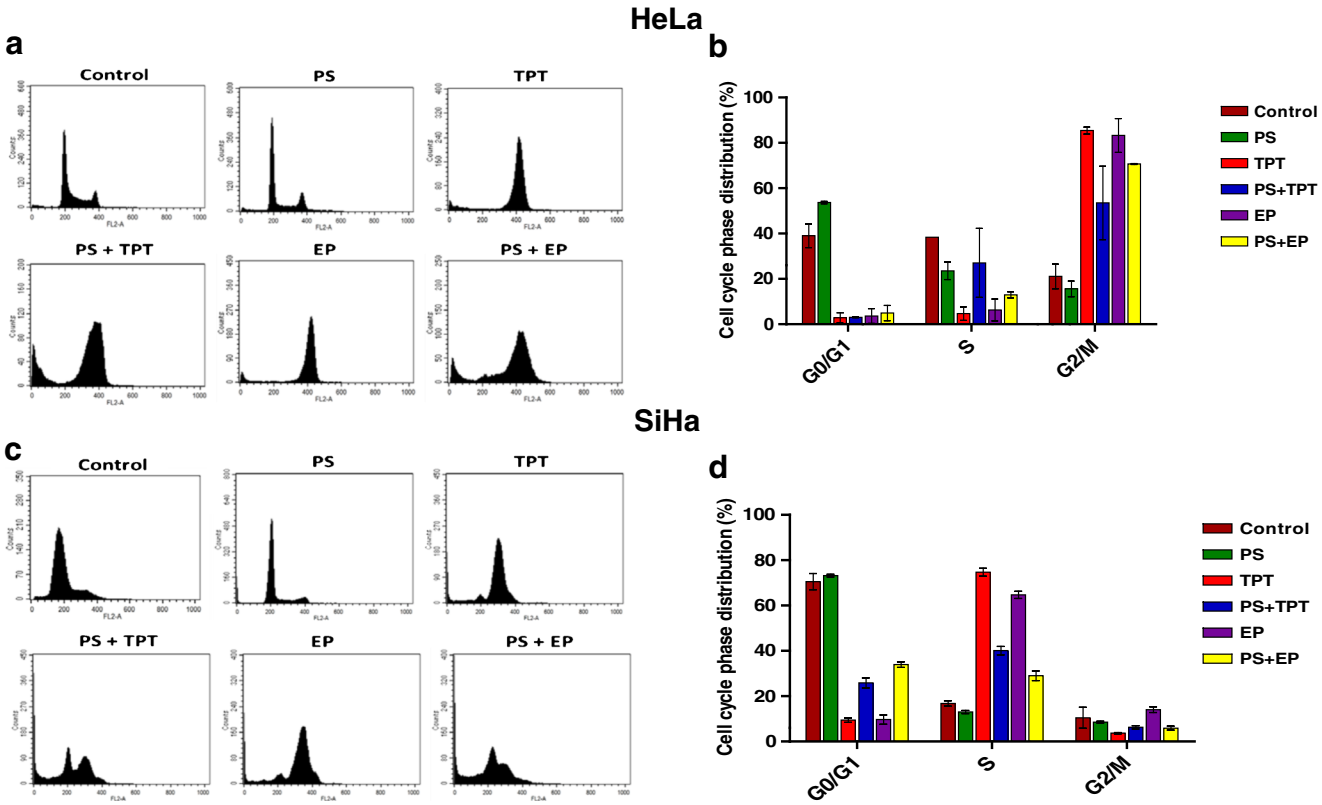

Fig. 2 Effect of panobinostat, topotecan and etoposide, alone or in combination, on the cell cycle kinetics of cervical cancer cells. Cells were treated with the IC_{50}^{72h} doses of various drugs alone or in combination and harvested after 24 h for FCM analysis after PI staining. Representative cell cycle plots of HeLa (**a**) and SiHa (**c**) cells are shown, including sub-G1 cell cycle phase distributions. Percent non-sub-G1 cell cycle phase distributions of HeLa (**b**) and SiHa (**d**) cells are shown. Each value is the mean ± SD of three independent experiments performed in triplicates. *PS*, panobinostat; *TPT*, topotecan; *EP*, etoposide

after combination treatment in both cell lines. Also, some cells with a red nucleus were observed after combination treatment, indicating necrotic cell death (Fig. S2a, b). Collectively, these results suggest that cell death occurred predominantly due to apoptosis rather than to necrosis, particularly when panobinostat was combined with topoisomerase inhibitors.

3.5 Increased apoptosis of cervical cancer cells after combined panobinostat and topoisomerase inhibitor treatment

To substantiate the above results quantitatively, the respective cells were again treated for 48 h and then analyzed by PI or Annexin V/PI double staining. In doing so, a significant increase in the percentage of hypodiploid sub-G1 cells after combination treatment of HeLa cells was observed (panobinostat: 21.6%; topotecan: 22%; etoposide: 24.1%; panobinostat + topotecan: 54.1%; panobinostat + etoposide: 43.2%), which is indicative of apoptotic cell death (Fig. 3a). Similarly, we found that in SiHa cells the percentage of sub-G1 cells increased significantly after combination treatment (panobinostat: 16.8%; topotecan: 21.7%; etoposide: 20.1%; panobinostat + topotecan: 42.8%; panobinostat + etoposide: 36.2%) (Fig. 3b). In addition, we found by Annexin V/PI staining that the percentage of viable cells was approximately 95% in the untreated control HeLa and SiHa cells (Fig. 3c, d). The percentage of apoptotic cells (both early and late) was found to be increased after single drug treatment with panobinostat, topotecan or etoposide (panobinostat: 18.5% (HeLa), 15% (SiHa); topotecan: 25.7% (HeLa), 28.8% (SiHa); etoposide: 25.6% (HeLa), 49.5% (SiHa), respectively. However, the percentage of apoptotic cells was significantly higher after combination treatment in both cell lines. The percentages of apoptotic cells were 49.8 and 44.3% for the panobinostat + topotecan combination in HeLa and SiHa cells, respectively. Similarly, we found that the panobinostat + etoposide combination resulted in 43.6 and 60.6% apoptotic cells in HeLa and SiHa cells, respectively. From these results, we conclude that combined treatment of cervical cancer cells with panobinostat and the topoisomerase inhibitors topotecan or etoposide synergistically increase apoptosis induction.

3.6 Combinations of panobinostat and topotecan or etoposide induce DNA damage of cervical cancer cells

Apoptotic cleavage of genomic DNA can be identified either by DNA fragments ('ladders') or by DNA smears after agarose gel electrophoresis. We found that in HeLa cells the DNA ladder patterns resulting from oligonucleosomal DNA cleavage were more pronounced after combination treatment. In SiHa cells, we found that the combination treatment resulted in DNA smear patterns. This smearing is known to be caused by cleavage of DNA into low molecular weight fragments that travel according to size on an agarose gel. The control cells did not show any DNA fragmentation (Fig. S3a, b). Thus, the data indicate that the combined treatment of cervical cancer cells with panobinostat and topotecan or etoposide results in DNA damage and, thereby, synergistic cell killing.

3.7 Synergistic apoptosis induction is correlated with enhanced ROS generation and mitochondrial dysfunction

In order to further delineate the mechanism(s) underlying the above observed enhanced synergistic apoptosis induction effects, we set out to assess alterations in ROS production and mitochondrial membrane potential. To this end, both cell lines were treated for 24 h with IC_{50}^{72h} doses of panobinostat, topotecan and etoposide, alone or in combination, after which ROS production was quantified by flow cytometry. We found that combinations of panobinostat and the topoisomerase inhibitors resulted in significant increases in ROS levels in both HeLa and SiHa cells, compared to single agent treated and untreated control cells (Fig. 4a, b). Addition of the free radical scavenger NAC (20 mM) significantly abrogated ROS accumulation induced by the combination treatment. The combination of panobinostat and topotecan resulted in 68.6% (HeLa) and 21.3% (SiHa) cells with an increased ROS production compared to the respective single drug treatments, i.e. panobinostat: 21.8% (HeLa), 11.9% (SiHa) and topotecan: 26% (HeLa), 12.6% (SiHa). The addition of NAC reduced the percentage of ROS generating cells to 34.4 and 6.9% in HeLa and SiHa, respectively. The combination of panobinostat and etoposide resulted in 52.5% (HeLa) and 24.8% (SiHa) cells with an increased ROS production compared to that of single drug treated cells, i.e., panobinostat: 21.8% (HeLa), 11.9% (SiHa) and etoposide: 21.2% (HeLa), 10.3% (SiHa). The addition of NAC reduced the percentage of ROS generating cells to 24.2 and 4.2% in HeLa and SiHa, respectively, in the combination treated group.

ROS generation is known to be associated with mitochondrial membrane potential (MMP) disruption, a critical event in apoptosis initiation, which can be measured by Rh 123 staining. We found that the percentage of cells treated with panobinostat, topotecan or etoposide alone showed low Rh 123 fluorescence intensities of 29.5, 34.2 and 37% in HeLa cells and 31.9, 29.2 and 56.9% in SiHa cells, respectively, compared to untreated controls (HeLa: 9.5%; SiHa: 14.3%). In addition, we found that the percentage of cells with a low Rh 123 fluorescence intensity increased significantly after combination treatment, i.e., the panobinostat + topotecan combination resulted in 50.5 and 58.7% Rh 123 negative HeLa and SiHa cells, respectively. Furthermore, we found that 57.5 and

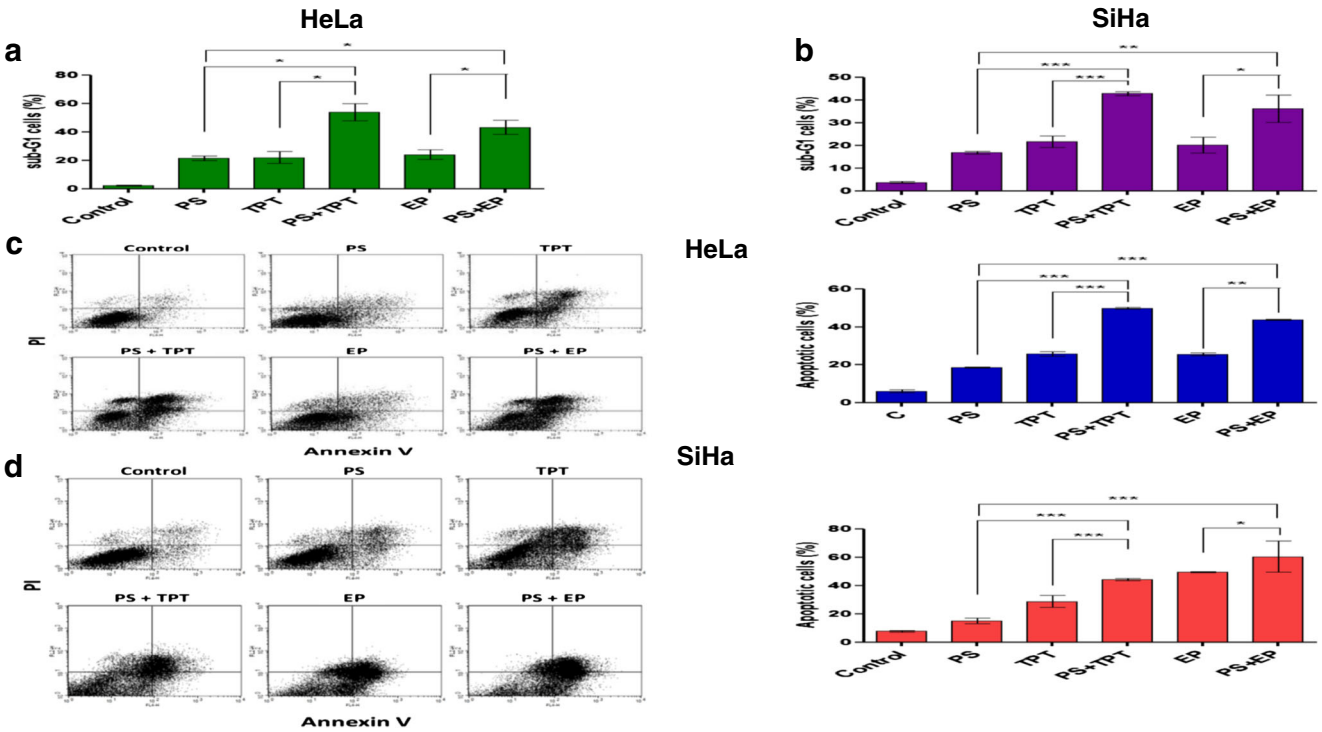

Fig. 3 Combination treatment of panobinostat with topoisomerase inhibitors potently enhances apoptosis in cervical cancer cells. HeLa (**a**, **c**) and SiHa (**b**, **d**) cells were treated with IC_{50}^{72h} doses of various drugs alone or in combination for 48 h. The cells were stained with PI and Annexin-V-APC/PI and analyzed using FCM. The percentages of sub-G1 HeLa (**a**) and SiHa (**b**) cells are shown. Representative FCM dot plots, early apoptotic (lower right quadrant) and late apoptotic (upper right quadrant) of HeLa (**c**) and SiHa (**d**) cells are shown. The percentages of apoptotic cells were quantified and are shown in parallel. The experiments were repeated thrice and the results are presented as mean ± SD of triplicates. *$p < 0.05$; ** $p < 0.01$; *** $p < 0.001$: combination treatment versus single drug treatment. *PS*, panobinostat; *TPT*, topotecan; *EP,* etoposide

68.3% HeLa and SiHa cells were Rh 123 negative following panobinostat + etoposide combination treatment, respectively (Fig. 4c, d). These results suggest that oxidative injury, resulting in disruption of mitochondrial membrane potential, may play a significant role in enhanced lethality induced by the combined treatment of cervical cancer cells with panobinostat and topotecan or etoposide.

3.8 Effect of combination treatment on the expression of apoptosis-related proteins in cervical cancer cells

In order to assess the expression of apoptosis-related proteins after combination treatment of panobinostat and topotecan or etoposide, Western blotting was performed. By doing so, we found that treatment with only panobinostat increased the expression of p21 in both cell lines, whereas individual treatment with the topoisomerase inhibitors topotecan or etoposide increased the expression of p21 only in SiHa cells. In addition, we found that the respective combined treatment regimens did not alter the expression pattern of p21 compared to the single drug treatments in either of the two cell lines (Fig. 5a, b). Bcl-2 family proteins are known to play critical roles in apoptosis by acting either as promoters (Bax) or as inhibitors (Bcl-2 and Bcl-xL) of the cell death process [10]. In order to further delineate the molecular mechanism(s) underlying apoptosis induction in cervical cancer cells, the expression of Bcl-2 family proteins after treatment with individual drugs or their combinations was investigated. Using Western blot analysis, we found that the combination treatment did not affect Bcl-2 expression in HeLa cells (Fig. 5a), whereas a significant decrease in Bcl-2 expression was observed in SiHa cells (Fig. 5b). Meanwhile, we found that the expression of another anti-apoptotic protein, Bcl-xL, was significantly decreased in both cell lines after combination treatment (Fig. 5a, b). The expression of Bax was found to be increased after combination treatment in both cell lines (Fig. 5a, b). Previously, it has been reported that once apoptosis promoters get activated due to loss of mitochondrial membrane potential, they may trigger caspase-mediated apoptotic cell death [11]. Therefore, we set out to assess the expression of caspase 9 and PARP in order to evaluate a putative induction of the intrinsic apoptotic pathway after combination treatment. We found that combined treatment of panobinostat with either one of the topoisomerase inhibitors induced the expression of both caspase 9 and cleaved PARP (Fig. 5a, b). These results indicate that the mitochondrial intrinsic apoptotic pathway is involved in the

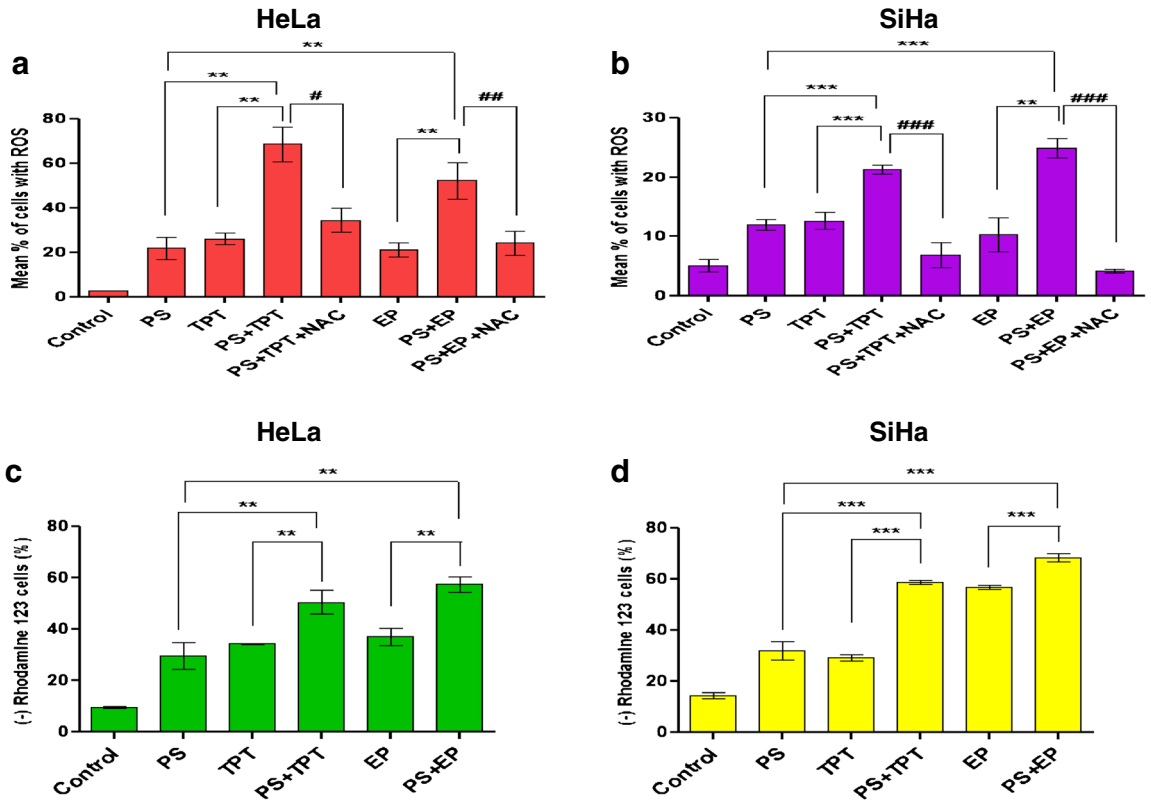

Fig. 4 Combination treatment of panobinostat and topoisomerase inhibitors synergistically result in ROS production and mitochondrial injury. The cells were treated with IC_{50}^{72h} doses of various drugs alone or in combination for 24 h, after which ROS generation was measured in HeLa (**a**) and SiHa (**b**) cells. The cells were also treated in the presence of NAC (20 mM), labeled with DCFH-DA and analyzed by FCM. MMP was determined using Rh 123 release in HeLa (**c**) and SiHa (**d**) cells. The data are expressed as mean ± SD from at least three independent experiments performed in triplicate. ** $p < 0.01$; *** $p < 0.001$: combination treatment versus single drug treatment. $^{\#}p < 0.05$; $^{\#\#}p < 0.01$; $^{\#\#\#}p < 0.001$: combination treatment versus combination treatment + NAC. *PS*, panobinostat; *TPT*, topotecan; *EP*, etoposide

synergistic interaction between panobinostat and the topoisomerase inhibitors topotecan or etoposide in cervical cancer cells.

3.9 Combination treatment affects the expression of proteins involved in survival signaling in cervical cancer cells

In addition to activation of the caspase cascade, also survival pathways are known to play a role in determining the fate of cells going through apoptosis. In order to further underscore the relevance of the above findings, we set out to investigate the effect of combination treatment (48 h) on the signaling proteins NF-κB, AKT and p-ERK. The choice of these proteins was based on their known role in survival signaling in cancer cells. In both cell lines declines in the NF-κB and AKT expression levels were observed after combination treatment with panobinostat and the topoisomerase inhibitors (Fig. 6a, b). ERK is a ubiquitous serine/threonine protein kinase that has been implicated in many cellular processes, including proliferation, survival and apoptosis. We observed a significant increase in the expression of (activated) p-ERK after combination treatment of both HeLa and SiHa cells (Fig. 6a, b). Together, these results suggest a model in which inhibition or activation of multiple signaling pathways may shift the balance of intracellular events towards apoptosis, thereby contributing to the observed efficacies of the combined treatment regimens tested.

4 Discussion

Combinations of molecular targeted therapies with conventional therapies are becoming mainstay in the treatment of various hematological and solid malignancies [12]. Since imbalances in the activity of HDACs can lead to gene expression deregulation, HDAC inhibitors (HDACi) have shown potential in anticancer therapies [13]. Panobinostat is a HDACi of the hydroxamic acid class of inhibitors and is FDA approved for the treatment of multiple myeloma in combination with bortezomib and dexamethasone. Currently, its potential efficacy is also being tested in combination with chemotherapeutic agents and small molecule inhibitors in solid tumors, and it has been found to have synergistic effects with doxorubicin,

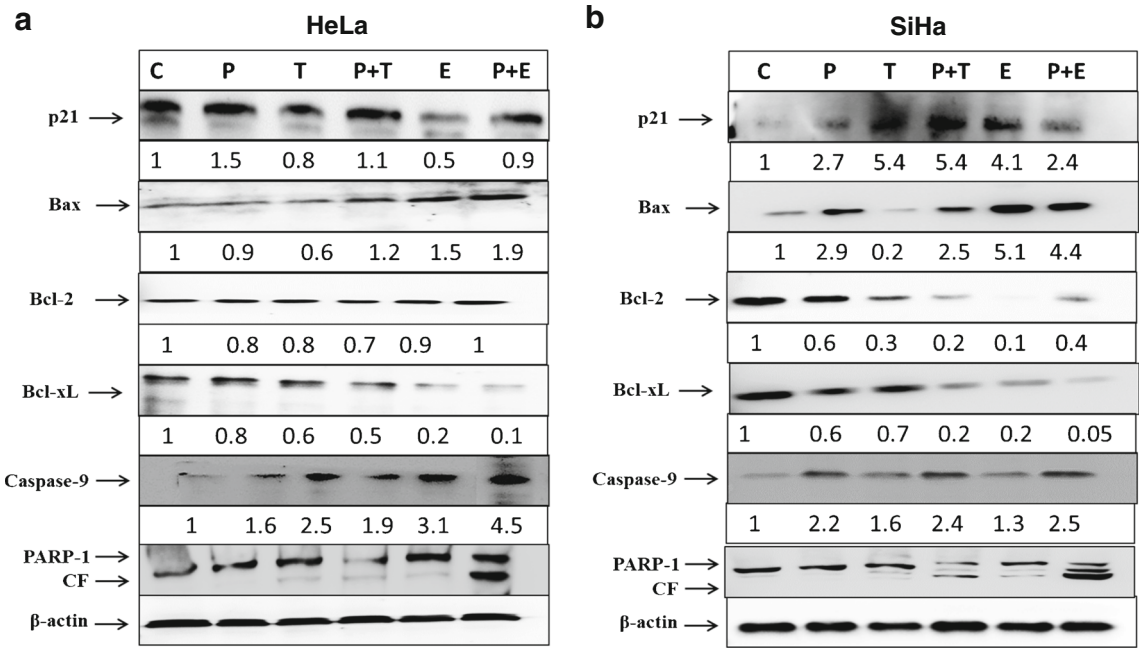

Fig. 5 Intrinsic apoptosis-related protein expression in cervical cancer cells after combination treatment. Representative blots of HeLa (**a**) and SiHa (**b**) cells are shown. The cells were treated with IC_{50}^{72h} doses of various drugs alone or in combination for 48 h. β-actin serves as loading control. The numbers below each lane refer to the fold-changes in protein level determined by densitometric analysis using ImageJ. The ratios of treated samples versus untreated controls following normalization for loading control are considered. *CF*, cleaved fragment; *C*, control; *P*, panobinostat; *T*, topotecan; *E*, etoposide

gemcitabine and docetaxel in both hormone receptor positive and negative breast cancer cells [14]. Panobinostat, which can alter DNA accessibility by regulating chromatin structure, has been found to exhibit synergistic effects with the FDA approved drug cisplatin for non-small cell lung cancer (NSCLC) [15], and the combination of panobinostat with the dual PI3K and mTOR inhibitor NVP-BEZ235 (BEZ235) has been found to induce apoptosis in human pancreatic ductal adenocarcinoma cells by attenuating p-AKT and Bcl-xL levels [16]. In addition, the combination of panobinostat with etoposide, doxorubicin or cisplatin has been found to result in enhanced synergistic antitumor effects in high-risk neuroblastoma cells [17].

Previously, we observed anticancer effects of panobinostat on cervical cancer cells, including synergistic effects with topoisomerase inhibitors [9]. These synergistic effects were found to be schedule-dependent, and the simultaneous combination treatment was found to be strongly synergistic with

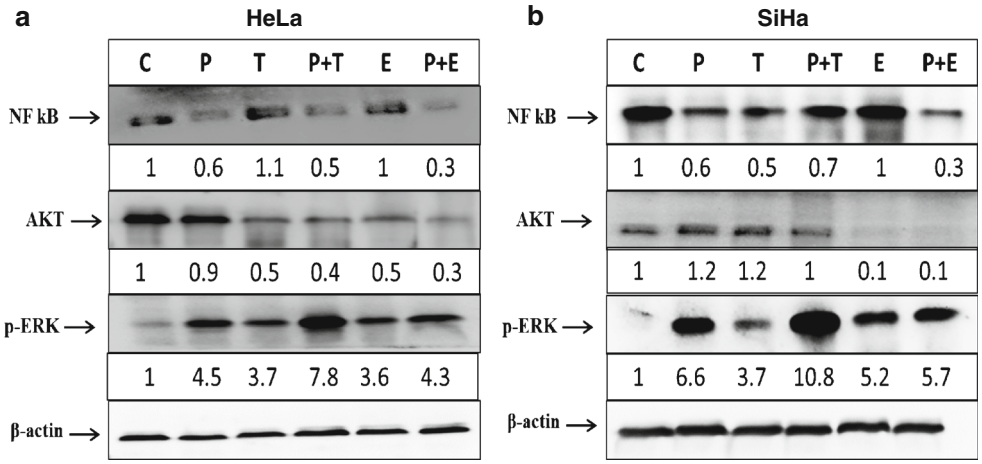

Fig. 6 Combination treatment of panobinostat and topoisomerase inhibitors synergizes with signaling pathways to induce apoptosis. Representative blots of HeLa (**a**) and SiHa (**b**) cells are shown. The cells were treated with IC_{50}^{72h} of various drugs alone or in combination for 48 h. β-actin serves as loading control. The numbers below lanes refer to the fold-changes in protein level determined by densitometric analysis using ImageJ. The ratios of treated samples versus untreated controls following normalization for loading control are considered. *C*, control; *P*, panobinostat; *T*, topotecan; *E*, etoposide

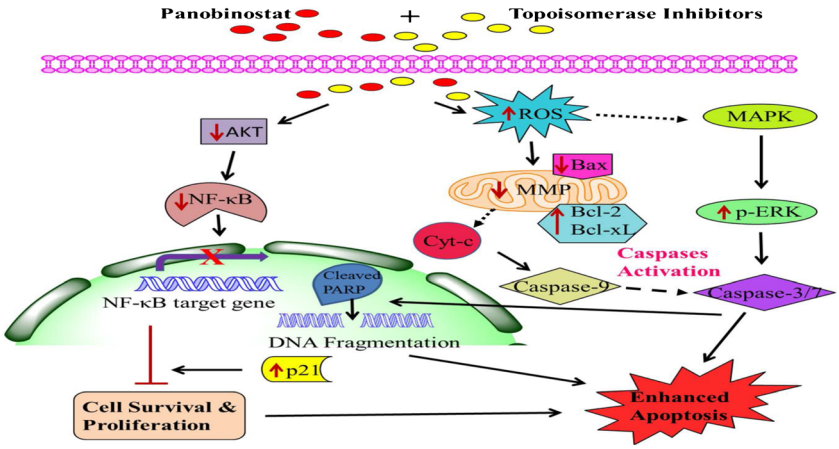

Fig. 7 Schematic overview of the mechanism of apoptosis induction by combination treatment of panobinostat and topoisomerase inhibitors in cervical cancer cells. The dotted arrows depict the activation of MAPK and the release of cytochrome c as reported in the literature. The dashed arrow depicts the activation of caspase 3/7 deduced from previous work

either of the two topoisomerase inhibitors tested, topotecan or etoposide. Here, we report on the molecular mechanisms underlying the synergistic anticancer effects exhibited by panobinostat combined with the topoisomerase inhibitors topotecan or etoposide on cervical cancer-derived HeLa and SiHa cells. We found that enhancement of apoptosis by the combination treatment serves as an important synergistic effect, but the underlying molecular mechanisms appeared to be diverse. Cell cycle analyses have previously shown that topotecan and etoposide may cause S or G2/M cell cycle arrest [17, 18], but this arrest was not abrogated in the simultaneous combination treatment in our study. This result indicates that panobinostat may not be able to disrupt or bypass cell cycle arrest induced by topotecan and/or etoposide.

To confirm the enhanced cell death elicited by synergistic interactions between panobinostat and the topoisomerase inhibitors, both qualitative and quantitative assays were performed. Apoptosis is known to be associated with distinct morphologic changes, including cell shrinkage, detachment from substratum, rounding of cells and membrane blebbing. These morphological changes were observed after combination treatment in both cervical cancer cell lines tested, thus suggesting apoptosis. Subsequently, AO/EB double staining and flow cytometry were used to substantiate the notion that the combination treatment-induced reduction in viability is indeed attributable to apoptosis. The results obtained revealed, both qualitatively and quantitatively, enhanced apoptosis after combination treatment in both HeLa and SiHa cells compared to single drug treatments. A scratch wound assay was used to assess the ability of these cervical cancer cells to migrate. The results showed that the speed of migration significantly decreased when panobinostat was combined with either topotecan or etoposide, compared to the untreated control and single drug-treated cells. These results support the synergistic mode of action of the combination treatment.

High levels of ROS can alter signaling pathways governing cellular growth, as well as apoptosis and/or necrosis [19]. Previous studies on various tumor cells have indicated that ROS generation represents an important mechanism by which panobinostat can exert its anticancer effects [9, 20]. In addition, it has been shown that topoisomerase inhibitors can increase the production of ROS in cancer cells [21]. Here, we found that ROS levels increased strikingly in cervical cancer cells exposed simultaneously to panobinostat and topoisomerase inhibitors. Notably, we found that the free radical scavenger NAC attenuated the oxidative stress imposed by ROS, suggesting a causal role for oxidative damage in the induction of apoptosis. We conclude that our data provide support for the notion that ROS generation is a crucial factor in panobinostat-topoisomerase inhibitor mediated apoptosis induction. To further elucidate the mechanism underlying the synergistic cytotoxicity of combination treatment, we assessed the effects of panobinostat and topotecan or etoposide on various apoptosis-related intracellular signaling proteins in HeLa and SiHa cells. It is well-documented that various factors can exert their anticancer effects via activation of the mitochondrial intrinsic apoptotic pathway. Mitochondria are both the source and target of ROS [22]. Excessive ROS production may lead to loss of the mitochondrial membrane potential (MMP), thereby causing leakage of apoptotic effectors [23]. The key element of the mitochondrial death pathway is the release of cytochrome c from mitochondria to the cytosol, where it is required for apoptosome assembly and activation of caspase 9 which, subsequently, leads to caspase 3 and 7 activation. Caspase 3 and 7, the executioners of the caspase family, cleave PARP, which is a characteristic feature of apoptosis. The anti-apoptotic Bcl-2 and Bcl-xL proteins can prevent these mitochondrial events, whereas the pro-apoptotic protein Bax can trigger them [24–26]. We found that the combined use of panobinostat and topotecan or etoposide triggers MMP disruption. We also found that the combination of panobinostat and topoisomerase inhibitors up-regulate Bax and down-regulate Bcl-2 and Bcl-xL expression levels in both cell lines. These shifts result in activation of the mitochondrial intrinsic apoptotic pathway through caspase 9 up-regulation. Previously, we observed enhanced caspase 3 and 7 activation during combination treatment [9], which

results in the formation of cleaved PARP and DNA fragmentation as observed in the present work. Therefore, we conclude that combination treatment increases ROS production and induces mitochondrial dysfunction and, ultimately, caspase-dependent apoptosis in cervical cancer cells.

The AKT/PKB (protein kinase B) pathway is an essential pathway for diverse cellular processes including survival, growth, proliferation, nutrient metabolism, transcription regulation, invasion and neo-vascularization. AKT is a serine-threonine kinase that mediates signaling pathways downstream of activated tyrosine kinases and phosphatidylinositol 3-kinase (PI3K). Over the past decade several studies have documented increased activation of AKT kinases in a variety of human solid tumors and hematological malignancies [27]. The PI3K/AKT pathway has also been shown to regulate NF-κB. The activation of NF-κB is dependent on phosphorylation of the IκB kinase (IKK) complex and degradation of IκB, an inhibitor of NF-κB. AKT activates IKK, a positive regulator of NF-κB, which causes phosphorylation and degradation of IκB. This leads to nuclear translocation and activation of NF-κB, where it can induce the transcription of anti-apoptotic genes [28, 29]. AKT also phosphorylates and directly antagonizes the action of the cell cycle inhibitor p21 [30]. The NF-κB transcription factors are best known for their role in promoting cell survival and antagonizing apoptosis, leading to tumorigenesis and chemo-resistance. The mechanism by which NF-κB promotes cell survival has been attributed, in part, to the up-regulation of anti-apoptotic genes of the Bcl-2 family such as Bcl-xL [31]. Notably, NF-κB also decreases ROS production, which is pivotal for apoptosis induction [32]. It has previously been shown that combinations of panobinostat and AEE788 (kinase inhibitor) or bortezomib result in inhibition of the AKT and NF-κB pathways in a variety of human cancer cell types [33]. Here, we show that the combined exposure of cervical cancer cells to panobinostat and topoisomerase inhibitors leads to down-regulation of the AKT and NF-κB protein levels. This observation suggests that inhibition of the PI3K/AKT and NF-κB pro-survival pathways may underlie the synergistic actions through which panobinostat and topotecan or etoposide induce apoptosis in cervical cancer cells.

Extracellular signal-regulated kinase (ERK) is a serine/threonine protein kinase that belongs to the family of mitogen-activated protein kinases (MAPKs). Mutation and deregulation of protein kinases play causal roles in human disease and provide a basis for developing agonists and antagonists that may be employed for therapy. Depending on the cell type and stimulus, ERK activity has been shown to mediate apoptosis. Several chemotherapeutic agents such as doxorubicin, etoposide and adriamycin, have been shown to activate ERK in various cancer cell lines. Oxidative stress due to increased accumulation of ROS induces activation of the Ras/Raf/ERK signaling pathway. Activation of the Ras/Raf/ERK pathway is, in turn, associated with the intrinsic apoptotic pathway, which is characterized by cytochrome c release from mitochondria and activation of the initiator caspase 9 [34–36]. The HDACi panobinostat has been shown to down regulate HDAC6 and to result in ERK activation in prostate cancer [37]. Here, we found that combination treatment of panobinostat and the topoisomerase inhibitors topotecan or etoposide results in increased expression of (activated) p-ERK, indicating up-regulation of the ERK pathway.

In conclusion, we report that panobinostat in combination with either topotecan or etoposide synergistically inhibits the growth of cervical cancer cells. Our data also indicate that this synergistic inhibition acts through ROS generation and activation of the mitochondrial intrinsic apoptotic pathway. ROS appears to be at the crossroad of both cell death and pro-survival pathways. Accordingly, we found that the combination treatment resulted in inhibition of the PI3K/AKT and NF-κB pro-survival pathways and in activation of the ERK pathway, which is associated with intrinsic apoptosis (Fig. 7). Our findings, which underscore a promising therapeutic potential of panobinostat/topoisomerase inhibitor combinations in cervical cancer, warrant further evaluation in appropriate preclinical cell and animal models to substantiate its putative clinical relevance.

Acknowledgements The authors wish to thank the University of Delhi, India, for providing funds in the form of a DUR&D grant and a UGC-SAP grant and UGC, New Delhi, India, for providing a fellowship to LW. We also wish to thank Mr. Prateek Arora for helping in FCM.

Compliance with ethical standards

Conflict of interest The authors declare no conflict of interest.

References

1. Y. Sun, Z. Sheng, C. Ma, K. Tang, R. Zhu, Z. Wu, R. Shen, J. Feng, D. Wu, D. Huang, D. Huang, J. Fei, Q. Liu, Z. Cao, Combining genomic and network characteristics for extended capability in predicting synergistic drugs for cancer. Nat Commun **6**, 8481 (2015). https://doi.org/10.1038/ncomms9481
2. S. Grant, Is the focus moving toward a combination of targeted drugs? Best Pract Res Clin Haematol **21**, 629–637 (2008). https://doi.org/10.1016/j.beha.2008.08.003
3. M. Bots, R.W. Johnstone, Rational combinations using HDAC inhibitors. Clin Cancer Res **15**, 3970–3977 (2009). https://doi.org/10.1158/1078-0432.CCR-08-2786
4. J. Gray, C.L. Cubitt, S. Zhang, A. Chiappori, Combination of HDAC and topoisomerase inhibitors in small cell lung cancer. Cancer Biol. Ther. **13**, 614–622 (2012). https://doi.org/10.4161/cbt.19848
5. A. Ferraro, Altered primary chromatin structures and their implications in cancer development. Cell Oncol **39**, 195–210 (2016). https://doi.org/10.1007/s13402-016-0276-6
6. L. Nolan, P.W. Johnson, A. Ganesan, G. Packham, S.J. Crabb, Will histone deacetylase inhibitors require combination with other

agents to fulfil their therapeutic potential? Br J Cancer **99**, 689–694 (2008). https://doi.org/10.1038/sj.bjc.6604557
7. M.S. Kim, M. Blake, J.H. Baek, G. Kohlhagen, Y. Pommier, F. Carrier, Inhibition of histone deacetylase increases cytotoxicity to anticancer drugs targeting DNA. Cancer Res **63**, 7291–7300 (2003)
8. K. Ozaki, F. Kishikawa, M. Tanaka, T. Sakamoto, S. Tanimura, M. Kohno, Histone deacetylase inhibitors enhance the chemosensitivity of tumor cells with cross-resistance to a wide range of DNA-damaging drug. Cancer Sci **99**, 376–384 (2008). https://doi.org/10.1111/j.1349-7006.2007.00669.x
9. L. Wasim, M. Chopra, Panobinostat induces apoptosis via production of reactive oxygen species and synergizes with topoisomerase inhibitors in cervical cancer cells. Biomed Pharmacother **84**, 1393–1405 (2016). https://doi.org/10.1016/j.biopha.2016.10.057
10. R.S. Hotchkiss, A. Strasser, J.E. McDunn, P.E. Swanson, Cell Death. N Engl J Med **361**, 1570–1583 (2009). https://doi.org/10.1056/NEJMra0901217
11. J.F. Kerr, C.M. Winterford, B.V. Harmon, Apoptosis. Its significance in cancer and cancer therapy. Cancer **73**, 2013–2026 (1994). https://doi.org/10.1002/1097-0142(19940415)73:8<2013::AID-CNCR2820730802>3.0.CO;2-J
12. K.T. Thurn, S. Thomas, A. Moore, P.N. Munster, Rational therapeutic combinations with histone deacetylase inhibitors for the treatment of cancer. Future Oncol **7**, 263–283 (2011). https://doi.org/10.2217/fon.11.2
13. O. Martinez-Iglesias, L. Ruiz-Llorente, R. Sanchez-Martinez, L. Garcia, A. Zambrano, A. Aranda, Histone deacetylase inhibitors: Mechanism of action and therapeutic use in cancer. Clin Transl Oncol **10**, 395–398 (2008). https://doi.org/10.1007/s12094-008-0221-x
14. D.R. Budman, A. Calabro, L. Rosen, M. Lesser, Identification of unique synergistic drug combinations associated with downexpression of survivin in a preclinical breast cancer model system. Anti-Cancer Drugs **23**, 272–279 (2012). https://doi.org/10.1097/CAD.0b013e32834ebda4
15. Y. Cai, X. Yan, G. Zhang, W. Zhao, S. Jiao, The predictive value of ERCC1 and p53 for the effect of panobinostat and cisplatin combination treatment in NSCLC. Oncotarget **6**, 18997–19005 (2015). https://doi.org/10.18632/oncotarget.3620
16. S. Venkannagari, W. Fiskus, K. Peth, P. Atadja, M. Hidalgo, A. Maitra, K.N. Bhalla, Superior efficacy of co-treatment with dual PI3K/mTOR inhibitor NVP-BEZ235 and pan-histone deacetylase inhibitor against human pancreatic cancer. Oncotarget **3**, 1416–1427 (2012). https://doi.org/10.18632/oncotarget.724
17. G. Wang, H. Edwards, J.T. Caldwell, S.A. Buck, W.Y. Qing, J.W. Taub, Y. Ge, Z. Wang, Panobinostat synergistically enhances the cytotoxic effects of cisplatin, doxorubicin or etoposide on high-risk neuroblastoma cells. PLoS One **8**, e76662 (2013). https://doi.org/10.1371/journal.pone.0076662
18. F. Bruzzese, M. Rocco, S. Castelli, E. Di Gennaro, A. Desideri, A. Budillon, Synergistic antitumor effect between vorinostat and topotecan in small cell lung cancer cells is mediated by generation of reactive oxygen species and DNA damage-induced apoptosis. Mol Cancer Ther **8**, 3075–3087 (2009). https://doi.org/10.1158/1535-7163.MCT-09-0254
19. D. Chen, J. Cao, L. Tian, F. Liu, X. Sheng, Induction of apoptosis by casticin in cervical cancer cells through reactive oxygen species-mediated mitochondrial signaling pathways. Oncol Rep **26**, 1287–1294 (2011). https://doi.org/10.3892/or.2011.1367
20. L. Gao, M. Gao, G. Yang, Y. Tao, Y. Kong, R. Yang, X. Meng, G. Ai, R. Wei, H. Wu, X. Wu, J. Shi, Synergistic activity of carfilzomib and Panobinostat in multiple myeloma cells via modulation of ROS generation and ERK1/2. Biomed Res Int **2015**, 459052 (2015)
21. O. Sordet, Q.A. Khan, I. Plo, P. Pourquier, Y. Urasaki, A. Yoshida, S. Antony, G. Kohlhagen, E. Solary, M. Saparbaev, J. Laval, Y. Pommier, Apoptotic topoisomerase I-DNA complexes induced by staurosporine-mediated oxygen radicals. J Biol Chem **279**, 50499–50504 (2004). https://doi.org/10.1074/jbc.M410277200
22. M.D. Brand, C. Affourtit, T.C. Esteves, K. Green, A.J. Lambert, S. Miwa, J.L. Pakay, N. Parker, Mitochondrial superoxide: Production, biological effects, and activation of uncoupling proteins. Free Radic Biol Med **37**(6), 755–767 (2004). https://doi.org/10.1016/j.freeradbiomed.2004.05.034
23. M. Ott, V. Gogvadze, S. Orrenius, B. Zhivotovsky, Mitochondria, oxidative stress and cell death. Apoptosis **12**, 913–922 (2007). https://doi.org/10.1007/s10495-007-0756-2
24. J.K. Brunelle, A. Letai, Control of mitochondrial apoptosis by the Bcl-2 family. J Cell Sci **122**, 437–441 (2009). https://doi.org/10.1242/jcs.031682
25. B. Leibowitz, J. Yu, Mitochondrial signaling in cell death via the Bcl-2 family. Cancer Biol Ther **9**, 417–422 (2010). https://doi.org/10.4161/cbt.9.6.11392
26. V.J. Bouchard, M. Rouleau, G.G. Poirier, PARP-1, a determinant of cell survival in response to DNA damage. Exp Hematol **31**, 446–454 (2003). https://doi.org/10.1016/S0301-472X(03)00083-3
27. D.A. Altomare, J.R. Testa, Perturbations of the AKT signaling pathway in human cancer. Oncogene **24**, 7455–7464 (2005). https://doi.org/10.1038/sj.onc.1209085
28. G. Song, G. Ouyang, S. Bao, The activation of Akt/PKB signaling pathway and cell survival. J Cell Mol Med **9**, 59–71 (2005). https://doi.org/10.1111/j.1582-4934.2005.tb00337.x
29. K. Vazquez-Santillan, J. Melendez-Zajgla, L. Jimenez-Hernandez, G. Martinez-Ruiz, V. Maldonado, NF-kappaB signaling in cancer stem cells: A promising therapeutic target? Cell Oncol **38**, 327–339 (2015). https://doi.org/10.1007/s13402-015-0236-6
30. F. Chang, J.T. Lee, P.M. Navolanic, L.S. Steelman, J.G. Shelton, W.L. Blalock, R.A. Franklin, J.A. McCubrey, Involvement of PI3K/Akt pathway in cell cycle progression, apoptosis, and neoplastic transformation: A target for cancer chemotherapy. Leukemia **17**, 590–603 (2003). https://doi.org/10.1038/sj.leu.2402824
31. M. Barkett, T.D. Gilmore, Control of apoptosis by Rel/NF-kappaB transcription factors. Oncogene **18**, 6910–6924 (1999). https://doi.org/10.1038/sj.onc.1203238
32. C. Bubici, S. Papa, C.G. Pham, F. Zazzeroni, G. Franzoso, The NF-kappaB-mediated control of ROS and JNK signaling. Histol Histopathol **21**, 69–80 (2006). https://doi.org/10.14670/HH-21.69
33. C. Yu, B.B. Friday, J.P. Lai, A. McCollum, P. Atadja, L.R. Roberts, A.A. Adjei, Abrogation of MAPK and Akt signaling by AEE788 synergistically potentiates histone deacetylase inhibitor-induced apoptosis through reactive oxygen species generation. Clin Cancer Res **13**, 1140–1148 (2007). https://doi.org/10.1158/1078-0432.CCR-06-1751
34. S. Cagnol, J.C. Chambard, ERK and cell death: Mechanisms of ERK-induced cell death–apoptosis, autophagy and senescence. FEBS J **277**, 2–21 (2010). https://doi.org/10.1111/j.1742-4658.2009.07366.x
35. Z. Lu, S. Xu, ERK1/2 MAP kinases in cell survival and apoptosis. IUBMB Life **58**, 621–631 (2006). https://doi.org/10.1080/15216540600957438
36. J.A. McCubrey, L.S. Steelman, W.H. Chappell, S.L. Abrams, E.W. Wong, F. Chang, B. Lehmann, D.M. Terrian, M. Milella, A. Tafuri, F. Stivala, M. Libra, J. Basecke, C. Evangelisti, A.M. Martelli, R.A. Franklin, Roles of the Raf/MEK/ERK pathway in cell growth, malignant transformation and drug resistance. Biochim Biophys Acta **1773**, 1263–1284 (2007). https://doi.org/10.1016/j.bbamcr.2006.10.001
37. M.J. Chuang, S.T. Wu, S.H. Tang, X.M. Lai, H.C. Lai, K.H. Hsu, K.H. Sun, G.H. Sun, S.Y. Chang, D.S. Yu, P.W. Hsiao, S.M. Huang, T.L. Cha, The HDAC inhibitor LBH589 induces ERK-dependent prometaphase arrest in prostate cancer via HDAC6 inactivation and down-regulation. PLoS One **8**, e73401 (2013). https://doi.org/10.1371/journal.pone.0073401